Clustering between AGNs and galaxies at high-redshifts

Masayuki Akiyama
(Astronomical Inst., Tohoku Univ.)
Hiroyuki Ikeda
(Kyoto Univ / Ehime Univ.)
Semi-analytic modeling team

HSC-AGN Ehime meeting 20121219

Schematic View of Growth History of Super Massive BHs

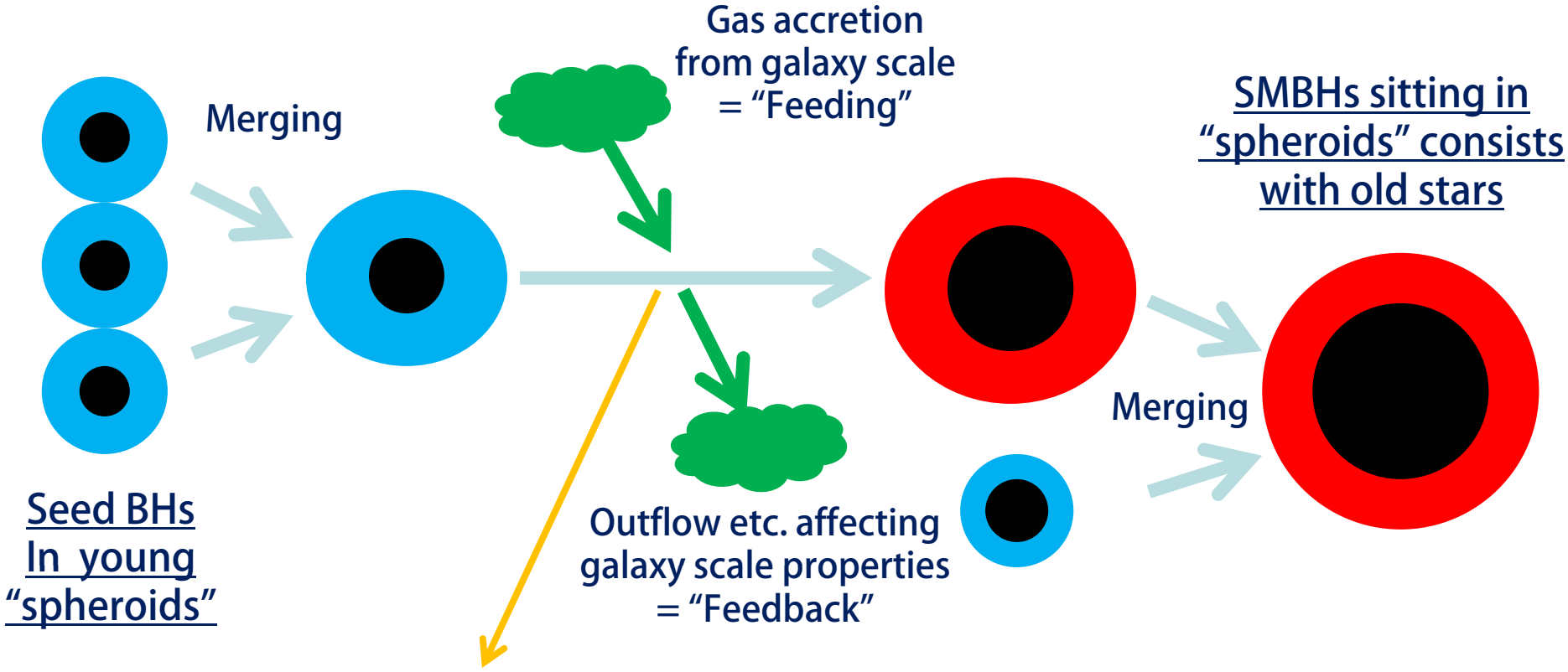

In order to qualitatively understand the growth history, for each SMBHs (or each population of SMBHs) we want to know

1. Accretion rate = Bolometric luminosity
2. BH Mass
3. Growth timescale = Accretion rate / BH Mass = Eddington ratio
4. Duty cycle = "QSO life time" Length of "QSO phase" in the life of galaxies

Background / Outline

0. Duty-cycle of QSOs in the early phase of their growth : before the peak of QSO activity, QSOs can be accreting at Eddington-limited manner with high-duty cycle ?

1. Examining clustering properties of QSOs at z~4 ?
   Can it be done only with the HSC-SSP dataset alone ?

2. By QSO-QSO clustering ?
   Can we examine the auto-correlation of QSOs of HSC-SSP dataset ?

3. By QSO-galaxy clustering ?
   Can we examine the cross-correlation between QSOs and galaxies ?

4. Beyond the clustering analysis ?

QSO-QSO auto-correlation strength and duty-cycle

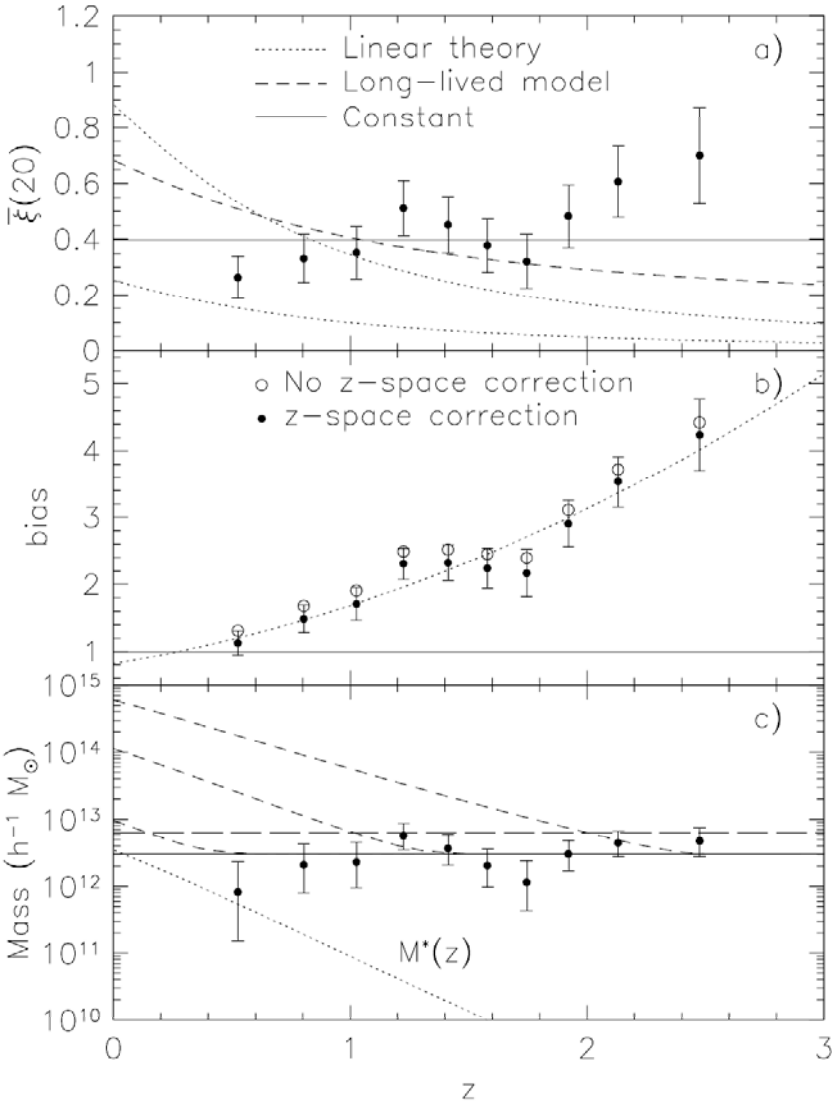

Croom et al. 2005

- QSO-QSO auto-correlation function (lower dotted line for CDM with WMAP cosmology)
- Bias = QSO clustering / CDM clustering
- Mean mass of dark matter halo of QSOs derived from the bias factor
- Dividing the number density of QSOs by the number density of the dark matter halos, duty-cycle of "QSO-phase" can be constraint.

QSO-QSO auto-correlation strength and duty-cycle

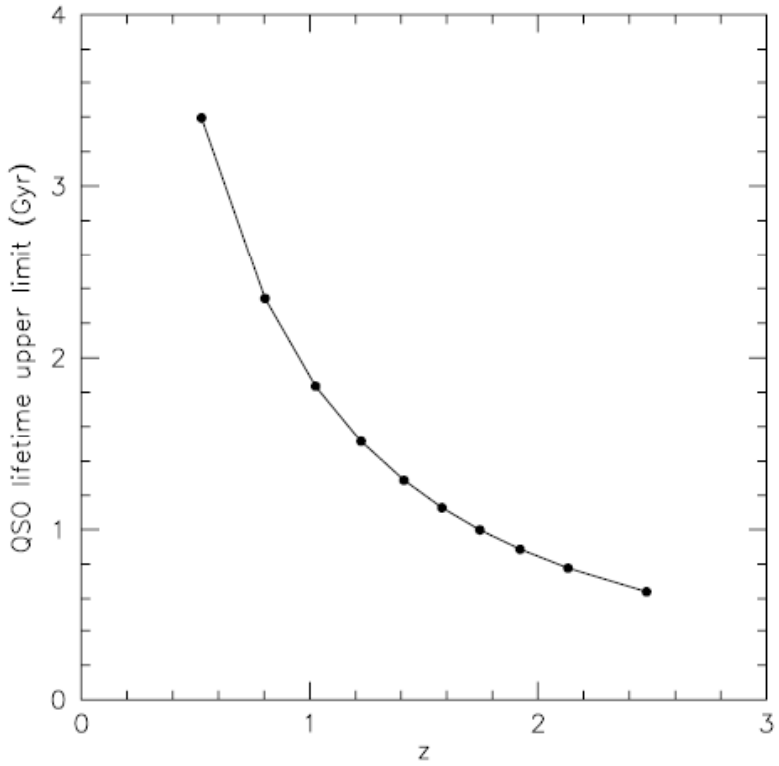

Figure 23. The 2σ upper limits to QSO lifetime as a function of redshift (connected filled circles), based on the growth in mass of DMHs.

Croom et al. 2005

- Upper limit for QSO lifetime is etimated with the time required for a dark matter halo with 3.0x10^12 Msolar (mean) to 6.2x10^12 Msolar (above 2sigma).

Results from QSO-QSO clustering at high-z

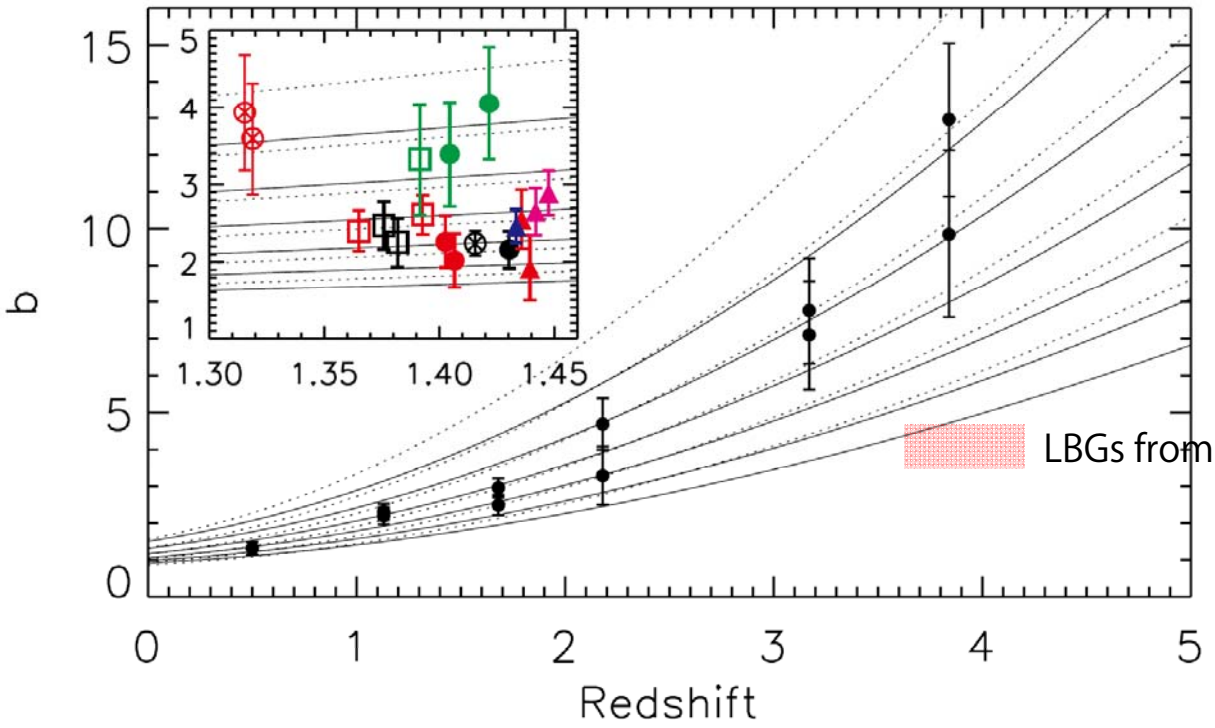

LBGs from Hildebrandt et al. 2009

- Stronger clustering of radio-loud QSOs
- The most luminous QSOs show stronger clustering.

Shen et al. 2009, ApJ, 697, 1656

Figure 12. Measured quasar bias factors for various samples. The filled circles in the main frame are results for all quasars within each redshift bin (no magnitude cut) and results both with and without negative data points in the fitting procedure are shown. The solid and dotted lines are halo bias factor evolution for fixed halo mass (from bottom to top) $M_{\rm halo} = 5 \times 10^{11}$, 1×10^{12}, 2×10^{12}, 4×10^{12}, 8×10^{12}, 1.6×10^{13} h^{-1} $M_\odot$ using the Sheth et al. (2001) and Jing (1998) fitting formulae, respectively. The Jing (1998) formula generally gives larger halo bias than the Sheth et al. (2001) formula for the same halo mass. In the inset, we show the quasar biases for our $0.4 < z < 2.5$ assembly samples divided by luminosity (filled circles: black for faint quasars, red for bright quasars, and green for the brightest quasars), virial mass (open squares: black for low-mass, red for high-mass, and green for the most massive quasars), color (filled triangles: blue for blue quasars, magenta for red quasars, and red for reddened quasars), and radio detection (circles with ×: black for FIRST-undetected quasars and red for FIRST-detected quasars). Their median redshifts have been shuffled to avoid clustering in the plot.

Locating "QSO-phase" in the evolutionally path of galaxies

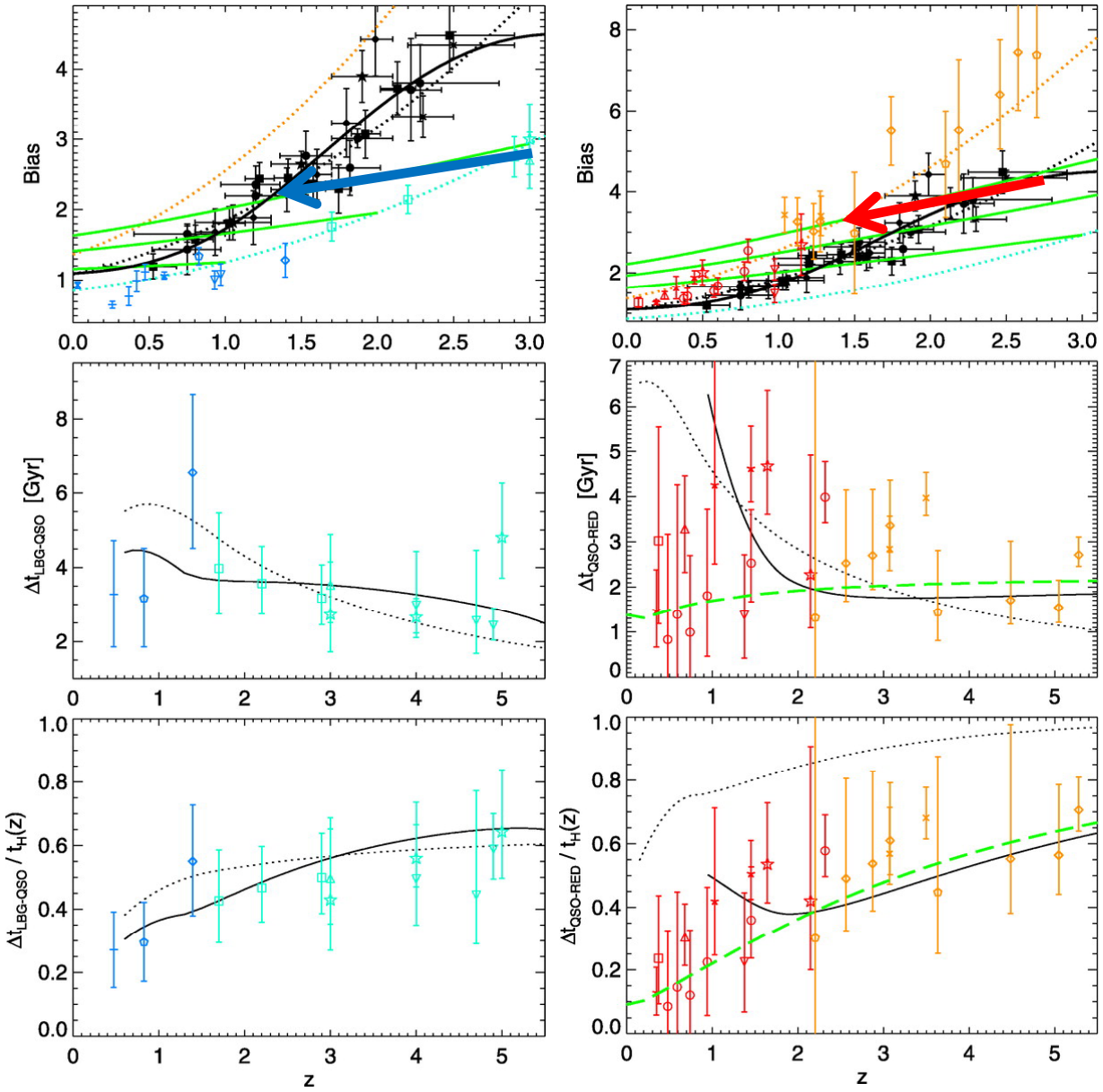

"QSOs", "blue starforming galaxies", and "red quiescent galaxies" are linked evolutionally through the measured clustering strength at each redshift.

"Blue starforming galaxies" with weak clustering are expected to evolve into "QSO" with stonger clustering, and further evolve into "red quiescent galaxies" with the strongest clustering.

The time-lag between the three phases are examined.

Hopkins et al. 2007

QSO auto-correlation in HSC survey only

- AGN-AGN auto-correlation function examined with the mock catalog from the semi-analytic model of Enoki et al.

  Quantitative examinations look difficult with imaging only AGN survey, especially at wide separation.

  Science target for PSF survey.

If we can divide z=3-4 QSO sample into 2 bins with zphot

If we have zspec

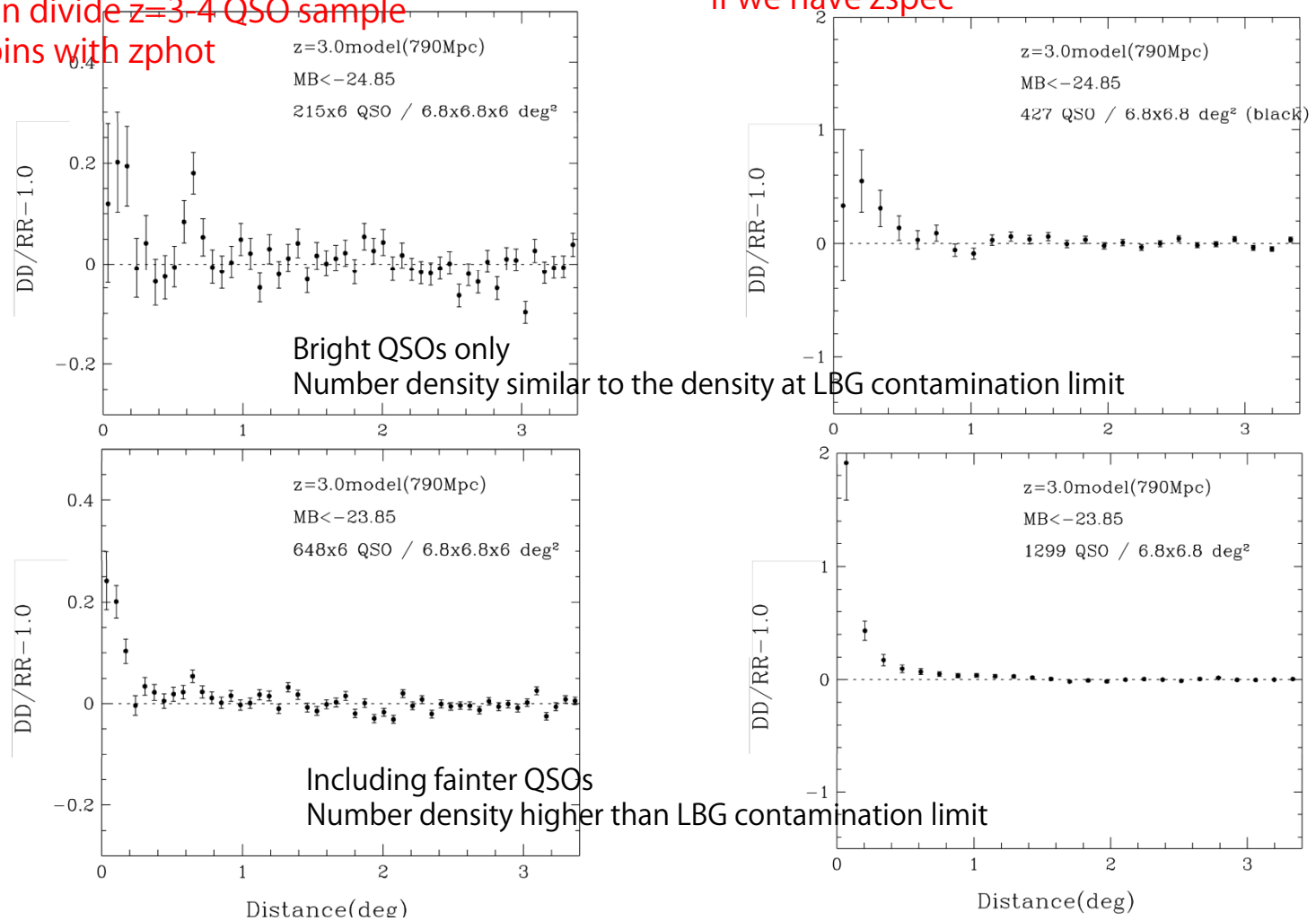

Bright QSOs only
Number density similar to the density at LBG contamination limit

Including fainter QSOs
Number density higher than LBG contamination limit

QSO-galaxy cross-correlation, instead ?

- Why AGN-AGN auto-correlation is difficult ?
  - The number of the pairs is not large enough to overcome the background/foreground contamination.

- Instead, AGN-galaxy cross-correlation function
  - At z~1 DEEP2 zspec: Coil et al. 2007
  - At z~1 AEGIS zspec: Coil et al. 2009

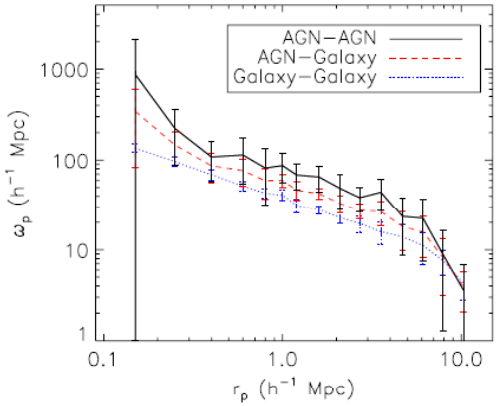

Figure 8. Projected AGN–galaxy cross-correlation function $w_p(r_p)$ as a function of scale for the nonquasar X-ray AGN main sample (red dashed line) and the full DEEP2 galaxy population in the EGS with $0.7 < z < 1.4$. The galaxy autocorrelation function in the same volume is shown (blue dotted line), as well as the inferred X-ray AGN autocorrelation function (black solid line). Errors are computed from jackknife samples of the data and are comparable to errors found from mock catalogs (see the text for details).

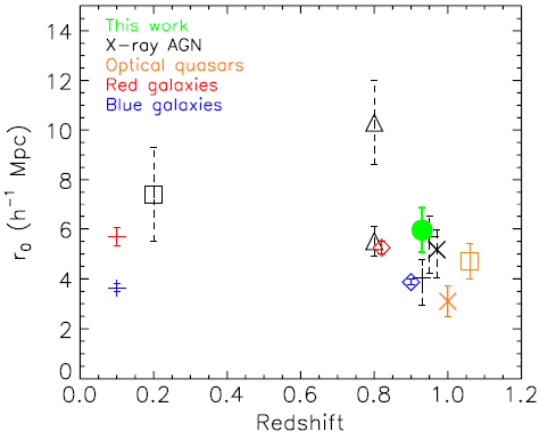

Figure 13. Clustering results for various AGN and galaxy surveys with $0 < z < 1$. The comoving correlation scale length, r_0, is plotted for different samples as a function of redshift. Shown in black with dashed line error bars are X-ray AGN clustering results from Mullis et al. (2004; open box), Gilli et al. (2005; triangle), Yang et al. (2006; plus sign), and Gilli et al. (2009; "X" sign). Results for X-ray AGN from this work are shown with a green filled circle. Results for red and blue galaxies are shown as red and blue markers for SDSS galaxies from Zehavi et al. (2005; plus sign) and DEEP2 galaxies from Coil et al. (2008; open diamond). At $z = 0.1$ galaxy clustering results from 2dF are similar to those shown for SDSS. Orange markers indicate measures of optically bright quasar clustering from Porciani et al. (2004; orange open box) and Coil et al. (2007; orange X sign). The clustering of X-ray AGN found in this paper shows that nonquasar X-ray AGNs cluster similarly to red galaxies at $z \sim 1$ and are more clustered than blue galaxies.

- At z=0.1-1.0 only with imaging dataset: Komiya-san, Shirasaki-san's poster

AGN-galaxy correlation at z~3

- At z~3 LBG – AGN: Adelberger & Steidel, 2005, ApJ, 630, 50

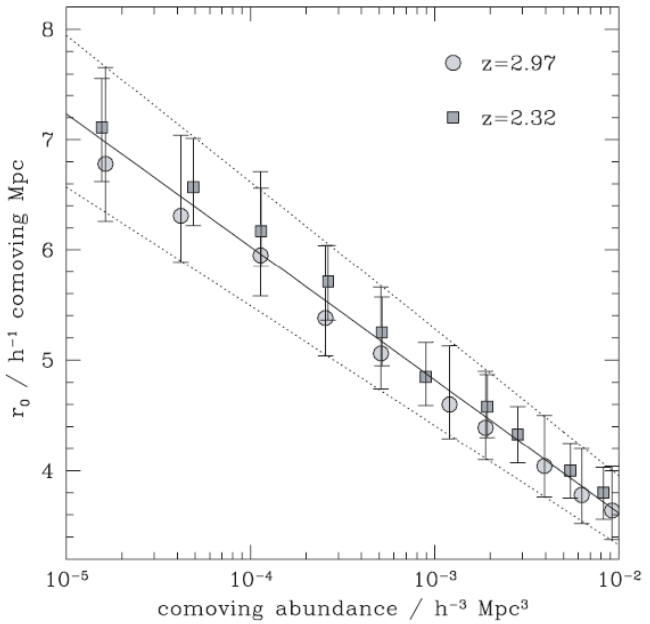

FIG. 4.—Theoretical relationship between the cross-correlation length r_0 and the AGN-halo comoving abundance n. Points show the GIF-ΛCDM relationship at two redshifts. The error bars indicate the uncertainty in the relationship due to the uncertainty in the galaxies' threshold mass. The solid line shows the least-squares compromise that we adopt throughout: $\log[n/(h^{-1}\ \mathrm{Mpc})^3] = -0.83 r_0 + 1.00$. The upper and lower dotted lines show the relationships that would result if we altered the assumed threshold mass by $\pm 1\ \sigma$. Fig. 6 shows that our conclusions would not be significantly affected if we adopted these relationships instead.

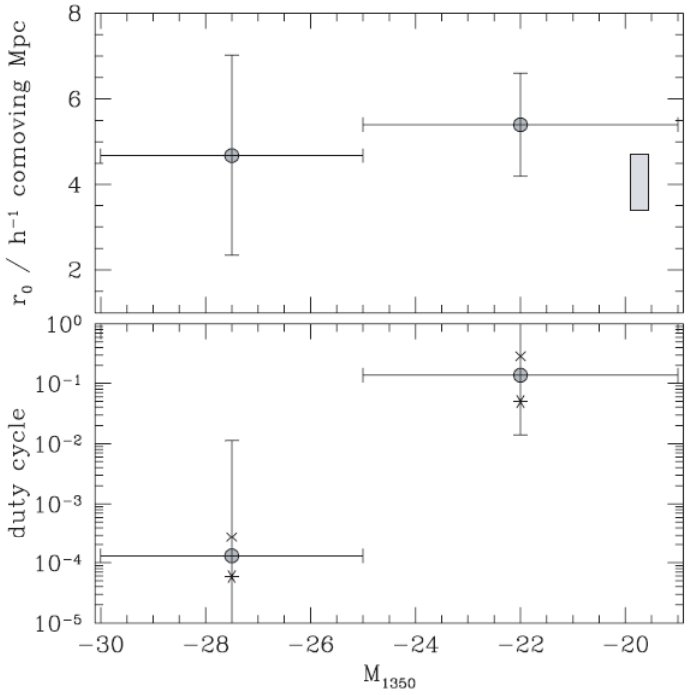

FIG. 6.—*Top*: Galaxy-AGN cross-correlation length as a function of AGN luminosity M_{1350}. Points with error bars show our measurements. The shaded rectangle shows the $\pm 1\ \sigma$ range of the galaxy-galaxy correlation length at similar redshifts (Adelberger et al. 2005a); its abscissa is arbitrary. *Bottom*: Implied duty cycle as a function of AGN luminosity. Error bars show the $\pm 1\ \sigma$ random uncertainty. The four- and six-pointed stars show how our estimated duty cycle would change if we altered the assumed relationship between clustering strength and abundance by an amount similar to its uncertainty. (They correspond to the upper and lower dotted envelopes in Fig. 4.) Note that the confidence intervals shown in this plot reflect only the constraints from our clustering analysis. Other considerations rule out a duty cycle of $\gtrsim 1$ for the faint AGNs and $\lesssim 10^{-5}$ for the bright AGNs, however. See § 5 for further discussion.

1st yr paper with 5-color 100 sq.deg dataset at "wide" depth

- "Locating luminous QSOs among luminous LBGs at z~4"
  - ~50 QSOs from SDSS sample with the same criteria with SMBH mass
    - Based on 3<z<5 QSOs brighter than i<20.5 = 1.37 /sq.deg (Richards et al. 2006, 131, 2766).
  - 400 QSOs with B-dropout selection method in 100 sq.deg, we may divide the sample with radio-loudness.
  - 1,000 (10,000) LBGs down to i=23 (24) in 100 sq.deg
  - 10deg corresponds to comoving 1200Mpc sufficiently big to trace the large scale distribution

Samples : AGNs

- HSC wide survey :
  - 1,000 sq.degree、5-bands
  - g(26.5), r(26.1), i(25.9), z(25.1), y(24.4) 5-sigma
  - g(27.5),r(27.1), i(26.9), z(26.1), y(25.4) 2-sigma

- AGNs
  - Imaging data only = g-dropout + morphology AGN/QSO selection
  - >4,000 QSOs at z=3.6-4.4 above r-mag<23.0 (LBG contamination limit) from Imanishi-san's summary

  - 1 deg. corresponds to comoving 120Mpc@z=3 - 136Mpc@z=4
  - 30 deg. corresponds to comoving 3600Mpc@z=3 – 4080Mpc@z=4

B-drop (g-drop) QSO selection

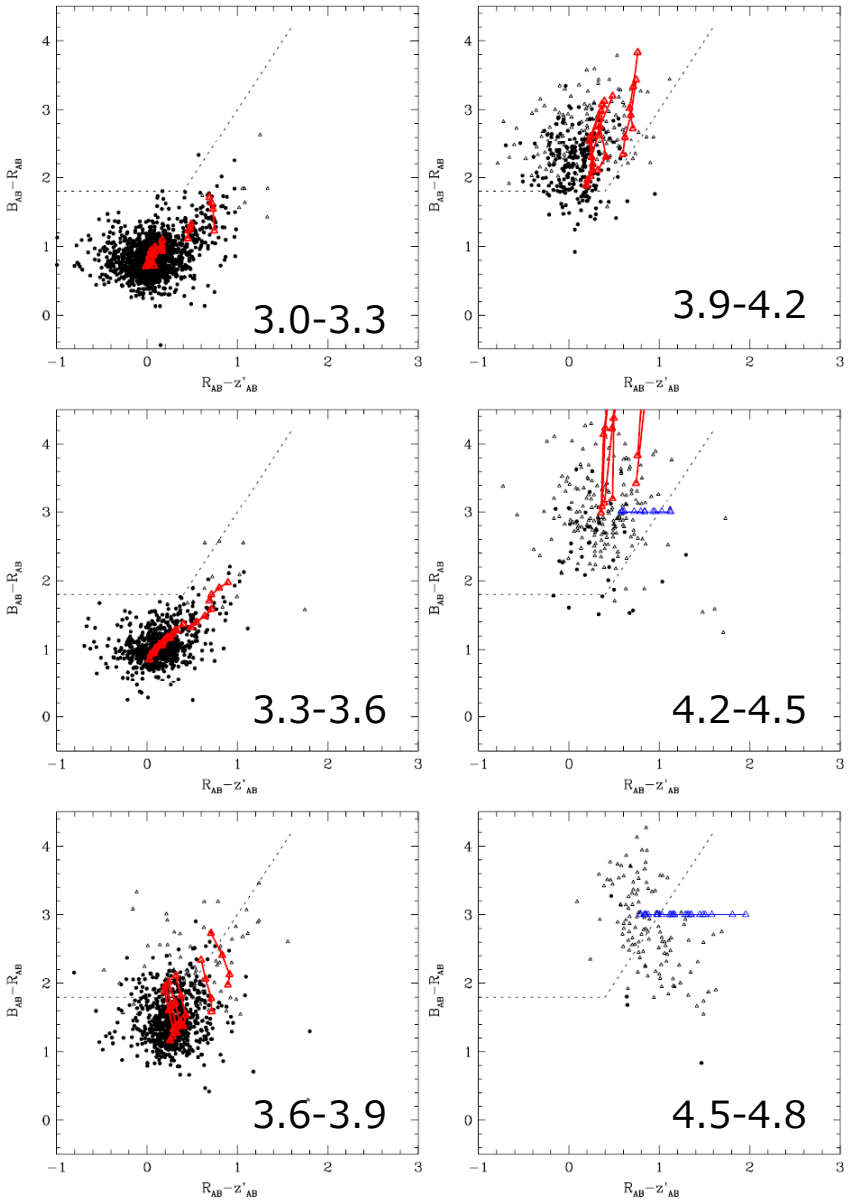

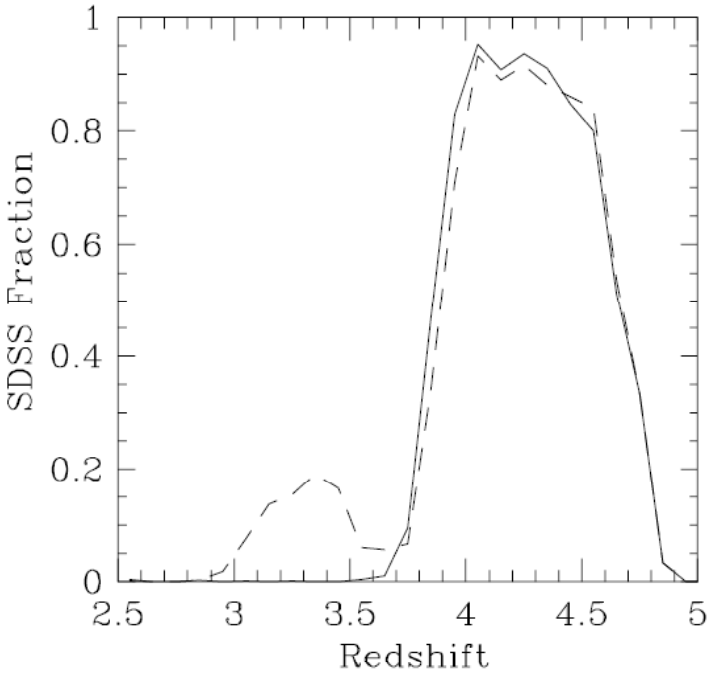

- Color distributions of SDSS spec-z QSOs as a function of redshift.
- The completeness function of QSOs (solid line) if we use the selection criteria shown with the dotted lines.
- Dashed line is the completeness function if we apply further reddening with E(B-V)=0.3
- See Ikeda-san's talk.

Samples: Galaxies

- Imaging data only = g-dropout selection of galaxies
  - >10 LBGs/sq.deg, >10,000 LBGs (luminous end) at z~4 above i-mag<23.0
  - >100 LBGs/sq.deg, >100,000 LBGs at z~4 above imag<24.0
  - Luminous LBGs are more extended than fainter LBGs, easier to be separated from QSOs ?

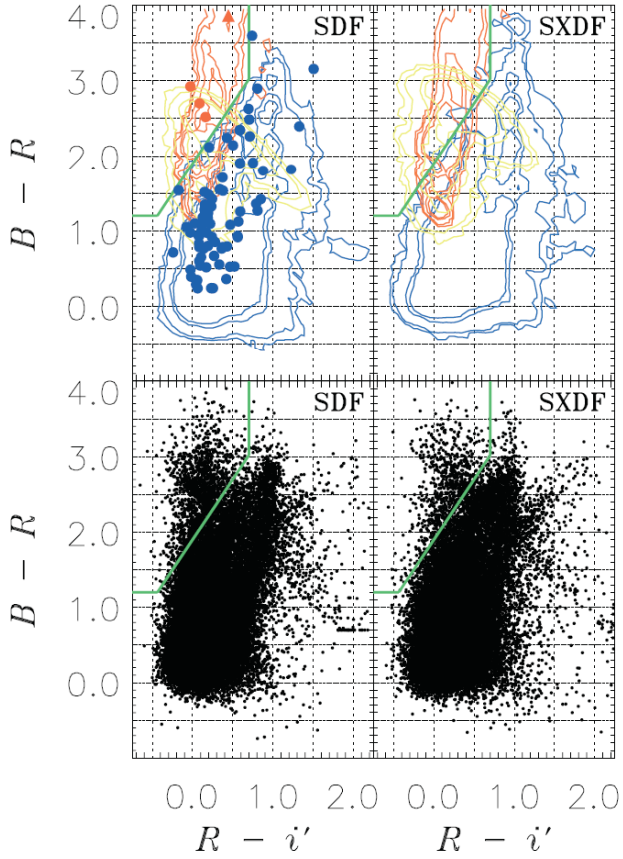

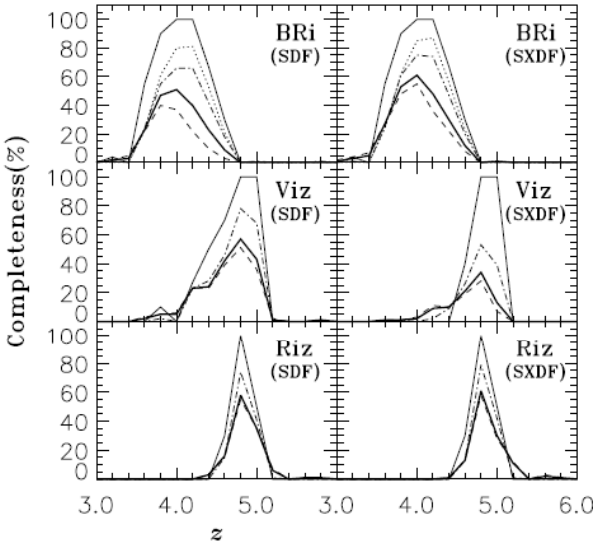

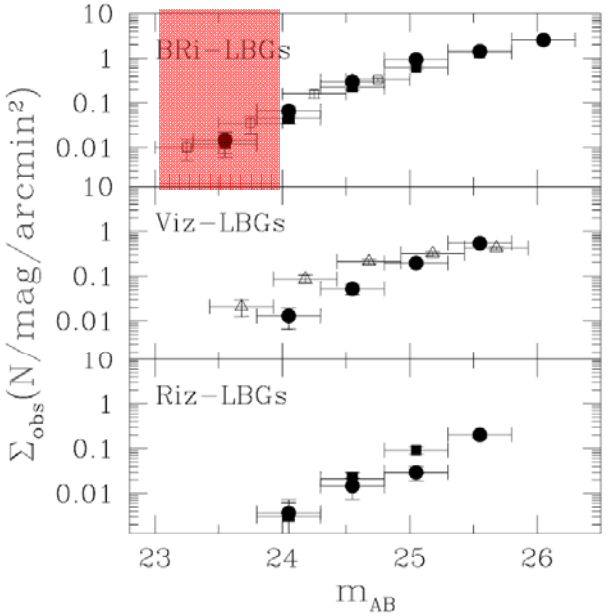

Ouchi et al. 2004, ApJ, 611, 660

FIG. 11.—Number counts of the LBGs selected in the SDF and SXDF. *BRi*-LBGs, *Viz*-LBGs, and *Riz*-LBGs are shown separately. The magnitude, m_{AB}, is the i'-band magnitude for *BRi*-LBGs and the z'-band magnitude for *Viz*-LBGs and *Riz*-LBGs. The circles and filled squares show data from the SDF and SXDF, respectively. Since the selection criteria for *Viz*-LBGs are different between the SDF and the SXDF, we do not plot data for *Viz*-LBGs in the SXDF to avoid confusion. Open squares (*top*) and triangles (*middle*) indicate the measurements for LBGs at $z \simeq 4$ and 5 obtained by Steidel et al. (1999) and Iwata et al. (2003), respectively. The number counts of our LBGs at $z \sim 4$ agree well with those of Steidel et al., while for *Viz*-LBGs a large discrepancy is seen at bright magnitudes between our measurements and those of Iwata et al. See the text for more details.

Samples: Galaxies

- Imaging data only = g-dropout selection of galaxies
  - >10 LBGs/sq.deg, >10,000 LBGs (luminous end) at z~4 above i-mag<23.0
  - >100 LBGs/sq.deg, >100,000 LBGs at z~4 above imag<24.0

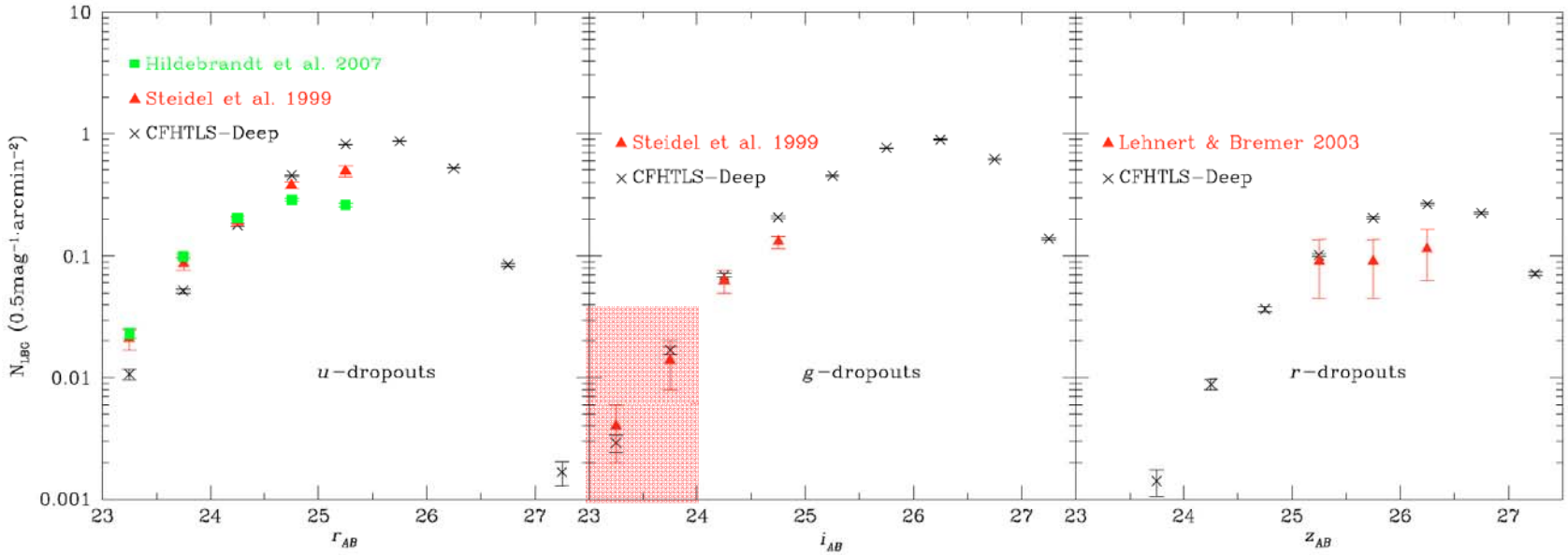

Fig. 4. Number counts for the three dropout samples (*u*-dropouts *left*, *g*-dropouts *middle*, and *r*-dropouts *right*) in the bands corresponding to approximately the same rest-frame UV-wavelength. We compare our *u*-dropout number counts to the ones from Steidel et al. (1999) and Hildebrandt et al. (2007) clearly showing the greater depth of the CFHTLS-Deep data. The *g*-dropout number counts are compared to Steidel et al. (1999) being consistent for $i < 24.5$ and suggesting some incompleteness of the older survey for fainter magnitudes. The 13 *R*-dropouts reported in Lehnert & Bremer (2003) show a similar number density as the *r*-dropouts in the current study.

Hildebrandt et al. 2009, A&A, 498, 725

B-drop “luminous” LBG

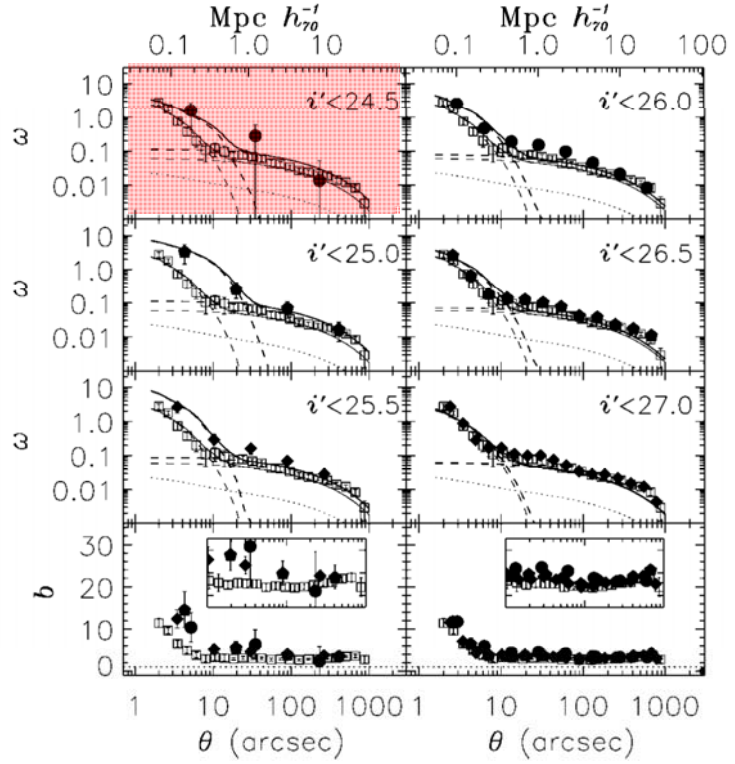

FIG. 3.—ACFs of magnitude-limited subsamples of LBGs at $z = 4.0$. In the top three panels, the filled symbols show the ACFs of our LBGs, with the limiting magnitude indicated in the legend. Each of these panels also shows the ACF of $i' < 27.5$ LBGs (*open squares*). The dotted curves are the ACF of dark matter predicted by the nonlinear model of Peacock & Dodds (1996). The thick solid and dashed lines indicate the best-fit ACFs of the halo model and the breakdown of 1 and 2 halo terms for each subsample, while the thin lines are for $i' <$ 27.5 LBGs. In the bottom panels, the biases of LBGs for each magnitude-limited subsample are shown by the same symbols as in the top three panels. The plots of large-scale biases are magnified in the inset boxes.

Ouchi et al. 2004, ApJ, 611, 660

- More luminous LBGs have stronger clustering.
- They trace the large scale structure more biased manner.

B-drop "luminous" LBG

	u-dropouts; $z_{\rm mean} = 3.16$						
$r_{\rm lim}$	$n_{\rm g}$ $[h^3\ {\rm Mpc}^{-3}]$	γ	r_0 $[h^{-1}\ {\rm Mpc}]$	$b_{\rm gal}$	IC	$\log\langle M_{\rm halo}\rangle$ $[h^{-1}\ M_\odot]$	$\langle N_{\rm g}\rangle$
24.5	$4.17 \times 10^{-4} \pm 4.24 \times 10^{-5}$	1.87 ± 0.07	6.16 ± 0.43	4.00 ± 0.26	0.0036	$12.68^{+0.20}_{-0.37}$	0.32 ± 0.27
25.0	$1.21 \times 10^{-3} \pm 1.21 \times 10^{-4}$	1.68 ± 0.03	4.39 ± 0.17	2.86 ± 0.09	0.0018	$12.26^{+0.19}_{-0.33}$	0.70 ± 1.02
25.5	$2.62 \times 10^{-3} \pm 2.63 \times 10^{-4}$	1.61 ± 0.02	3.54 ± 0.10	2.39 ± 0.05	0.0013	$12.06^{+0.13}_{-0.19}$	0.84 ± 0.66
$i_{\rm lim}$	g-dropouts; $z_{\rm mean} = 3.76$						
25.0	$3.41 \times 10^{-4} \pm 3.46 \times 10^{-5}$	1.94 ± 0.08	6.02 ± 0.43	4.57 ± 0.36	0.0028	$12.39^{+0.10}_{-0.13}$	0.45 ± 0.33
25.5	$8.68 \times 10^{-4} \pm 8.73 \times 10^{-5}$	1.68 ± 0.08	5.24 ± 0.30	3.78 ± 0.19	0.0019	$12.17^{+0.06}_{-0.07}$	0.65 ± 0.57
26.0	$1.76 \times 10^{-3} \pm 1.76 \times 10^{-4}$	1.70 ± 0.04	4.16 ± 0.16	3.12 ± 0.10	0.0013	$12.08^{+0.05}_{-0.06}$	0.48 ± 0.13
$z_{\rm lim}$	r-dropouts; $z_{\rm mean} = 4.73$						
25.5	$2.27 \times 10^{-4} \pm 2.34 \times 10^{-5}$	2.10 ± 0.07	7.10 ± 0.53	6.95 ± 0.57	0.0108	$12.26^{+0.12}_{-0.17}$	0.30 ± 0.18
26.0	$5.40 \times 10^{-4} \pm 5.46 \times 10^{-5}$	2.13 ± 0.07	5.53 ± 0.26	5.41 ± 0.29	0.0066	$12.08^{+0.16}_{-0.25}$	0.39 ± 0.26
26.5	$9.49 \times 10^{-4} \pm 9.56 \times 10^{-5}$	2.09 ± 0.04	4.71 ± 0.17	4.52 ± 0.17	0.0046	$12.00^{+0.13}_{-0.19}$	0.16 ± 0.20

Hildebrandt et al. 2009, A&A, 498, 725

Clustering between AGNs and galaxies at z~4

Projected cross-correlation of model AGNs (randomly selected 200 galaxies with M*>10^10.5, 10^10, 10-9 Msolar) and model galaxies (10,000 galaxies with M*>10^10 Msolar) at z~4 based on the mock catalogs of AGNs and galaxies from semi-analytic model of Enoki et al.
Available volume of the model corresponds to the survey area of 3.2x3.2 deg^2 (400x400 Mpc^3 comoving volume).

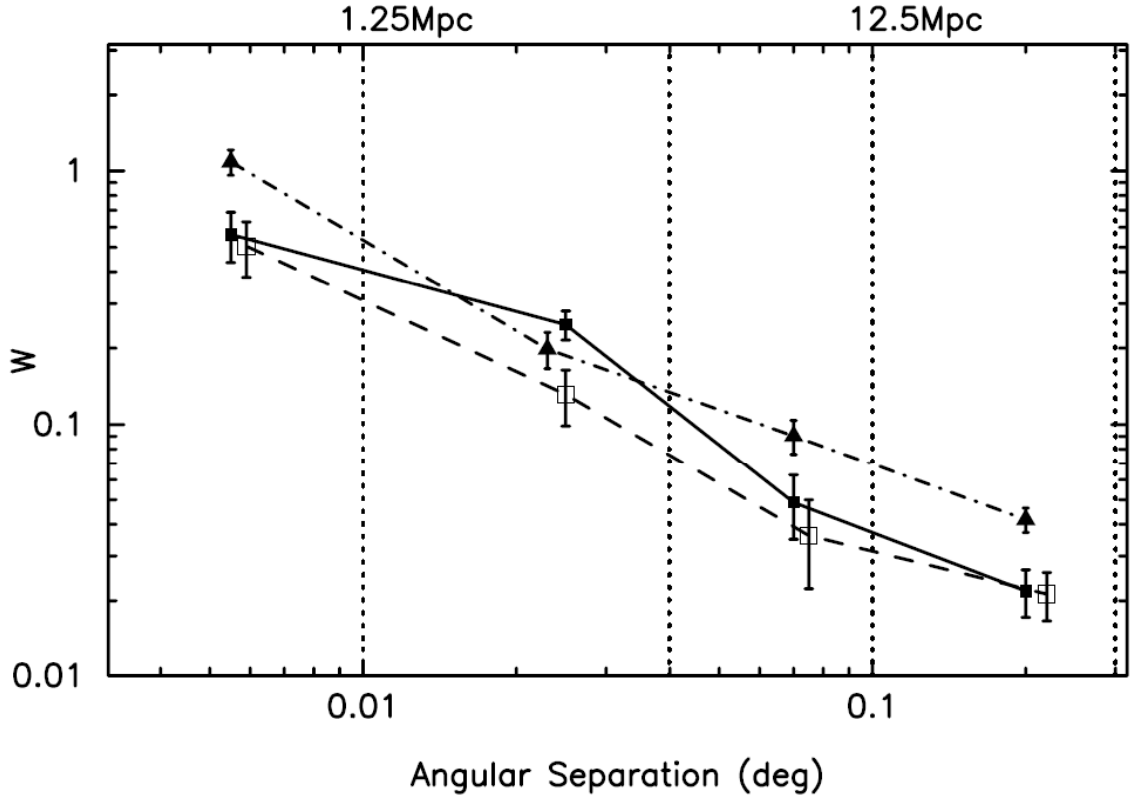

Beyond clustering analysis ? I.

- How about locate (bright) AGNs in the large scale structure of the high-redshift universe efficiently traced with luminous LBGs ?
- Using the "luminous" LBGs sample, we can identify density peaks of galaxies effectively. Then, we can examine the association of QSOs with the density peaks of LBGs.
- That can be the direct constraints on the Halo Occupation Distribution.

HOD from the fraction of AGNs among X-ray selected groups of galaxies at z<1: Allevato et al. 2012

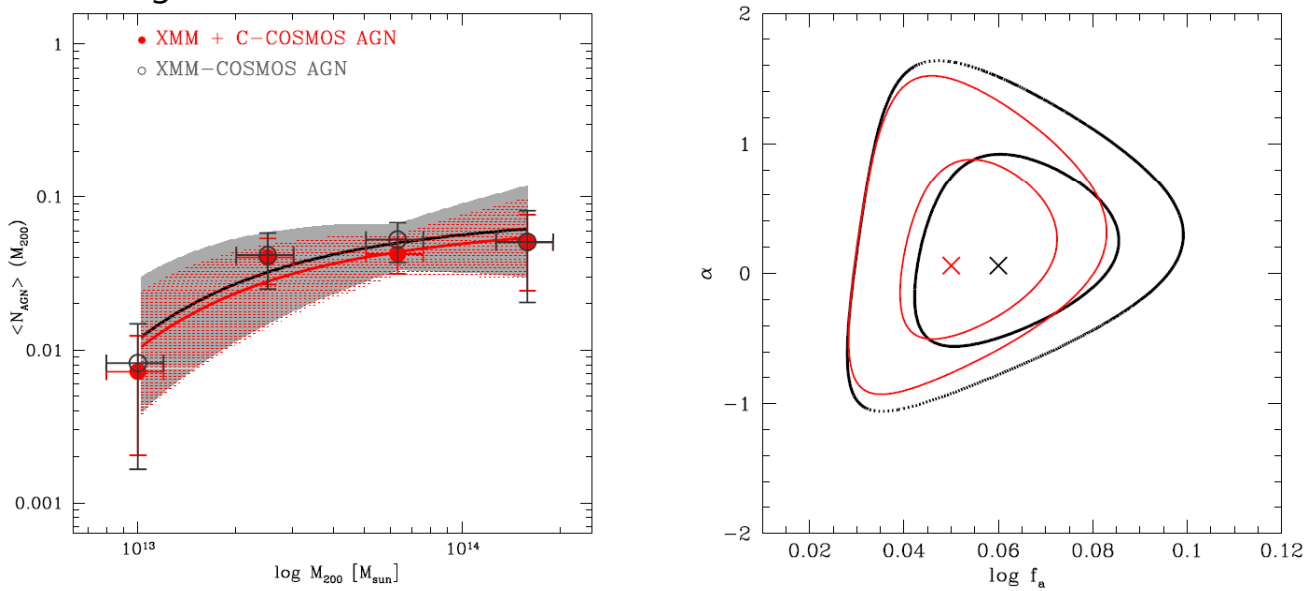

FIG. 4.— *Left Panel*: Occupation of galaxy groups by 41 XMM-COSMOS AGN (black open circles) and 58 XMM + C-COSMOS AGN (red filled circles) as a function of the halo mass, when correcting for the XLF and for the redshift evolution of the AGN density. The fit assuming a rolling-off power-law dependence of the HOD is shown as the solid black lines (best fit) and shaded regions (1σ confidence interval, $\Delta\chi^2 = 2.3$). *Right Panel*: the confidence contours of the power-law best-fit parameters α and f_a, for XMM-COSMOS AGN

Beyond clustering analysis ? II.

- AGN feedback and habitat segregation ? (Kashikawa et al. 2007)
  - Association of a QSO and LBGs filament,
  - no excess of LAEs = effect of QSO feedback ?
    - Also in Bruns et al. 2012
  - Can be examined with fainter LBG sample in stead of LAE ?

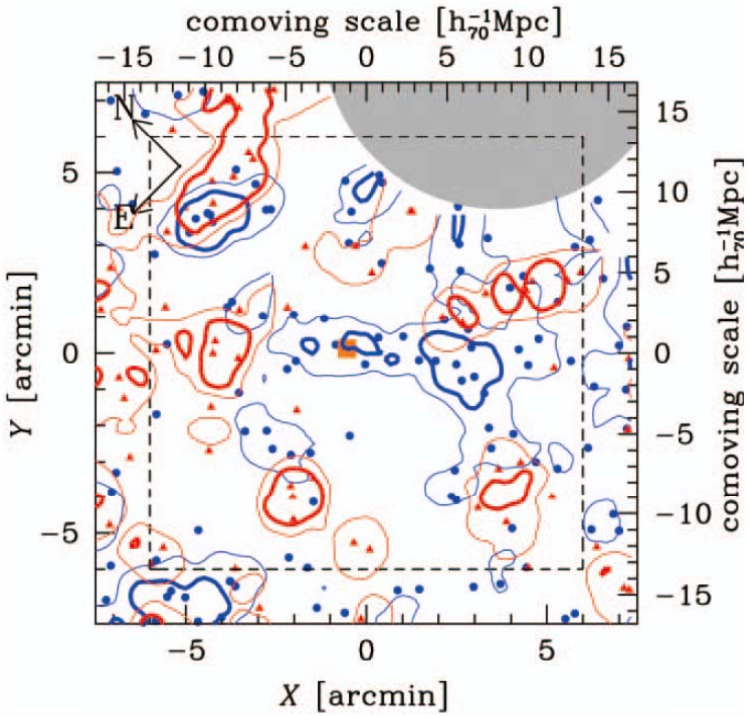

FIG. 4.—LAA (*blue circles*)/ LAE (*red triangles*) distribution and its surface number density contours (blue for LAAs and red for LAEs) in the QSO field around SDSS J0211−0009 (*central orange square*). The QSO field is defined as a 12×12 arcmin^2 region, indicated by dashed lines. The thin and thick contours

Summary

0. Duty-cycle of QSOs in the early phase of their growth : before the peak of QSO activity (at z~2-3), QSOs can be accreting at Eddington-limited manner with high-duty cycle ?

1. Duty-cycle or QSO lifetime from QSO clustering
   It looks difficult to examine the auto-correlation of QSOs with HSC-SSP dataset alone ?
   Good science case with PFS !

2. Duty-cycle from QSO-galaxy clustering
   We can examine the cross-correlation between QSOs and galaxies with HSC-SSP dataset.

3. Beyond the clustering analysis ?
   QSO association with LBG clusters = Halo Occupation Distribution
   QSO feedback to small galaxies